

# Influences of nanocarrier morphology on therapeutic immunomodulation

Molly Frey<sup>1</sup>, Sharan Bobbala<sup>2</sup>, Nicholas Karabin<sup>2</sup> & Evan Scott<sup>\*,1,2,3,4,5</sup>

<sup>1</sup>Interdisciplinary Biological Sciences Program, Northwestern University, Evanston, IL 60208, USA

<sup>2</sup>Department of Biomedical Engineering, Northwestern University, Evanston, IL 60208, USA

<sup>3</sup>Chemistry of Life Processes Institute, Northwestern University, Evanston, IL 60208, USA

<sup>4</sup>Simpson Querrey Institute, Northwestern University, Chicago, IL 60611, USA

<sup>5</sup>Robert H. Lurie Comprehensive Cancer Center, Northwestern University, Chicago, IL 60611, USA

\*Author for correspondence: [evan.scott@northwestern.edu](mailto:evan.scott@northwestern.edu)

Nanomaterials provide numerous advantages for the administration of therapeutics, particularly as carriers of immunomodulatory agents targeting specific immune cell populations during immunotherapy. While the physicochemical characteristics of nanocarriers have long been linked to their therapeutic efficacy and applications, focus has primarily been placed on assessing influences of size and surface chemistry. In addition to these materials properties, the nanostructure morphology, in other words, shape and aspect ratio, has emerged as an equally important feature of nanocarriers that can dictate mechanisms of endocytosis, biodistribution and degree of cytotoxicity. In this review, we will highlight how the morphological features of nanostructures influence the immune responses elicited during therapeutic immunomodulation.

**Lay summary:** Nanotechnology has become a key tool for the controlled delivery of drugs and therapeutics. The shape and structure of these nanoscale drug carriers strongly influence their effectiveness for targeting specific cells and organs of the immune system. Here, we discuss numerous examples in the recent literature where the shape and structure of such nanocarriers has been found to be advantageous for directing immune responses during vaccination and immunotherapy.

First draft submitted: 13 February 2018; Accepted for publication: 3 May 2018; Published online: 7 August 2018

**Keywords:** antigen-presenting cells • biodistribution • drug delivery • immunomodulation • immunotherapy • nanocarrier • nanomaterial • nanoparticle • theranostics • vaccination

The innate and adaptive immune systems have undergone significant evolutionary developments in response to the selective pressure of pathogens [1,2,3]. As pathogens mutate to increase virulence and pathogenicity, the targeted host immune system must also adapt to these changes in order to maintain survival and preservation of the species. Indeed, this arms race has produced increasingly complex pathogenic strategies to evade [4] and manipulate [5,6] both host immune components as well as targeted antimicrobial drugs [7–9]. Among these strategies is developing diverse morphologies to impact immune recognition, uptake and penetration of microbes and virions into host cells, with many strains known to switch between several polymorphic states based on environmental conditions [10,11]. Taking into consideration the vast diversity of pathogen morphology, it may prove advantageous to incorporate rationally selected structural elements when therapeutically targeting immune system components with nanoscale vehicles.

Morphological plasticity significantly enhances pathogen survival and virulence by combining the benefits of multiple shapes for a greater range of context. Fungal species are known for switching between filamentous hyphae and spherical yeast forms, while influenza produces filamentous and spherical components that are internalized by distinct mechanisms [12]. *Escherichia coli* form rod structures when penetrating host cells but switch to filaments to enhance escape from successfully infected cells [13]. The filamentous worm-like structure is noted in organisms such as *Legionella*, *Borrelia*, Ebola and Marburg, with the latter two belonging to the viral family Filoviridae in reference to the filamentous morphology of their virions. Using *Legionella* as a model structure, filaments were shown to delay phagosome sealing thereby interfering with the acidification of phagosomes needed for maturation,

endosome fusion and subsequent antimicrobial lysis [14]. Bacilli such as *B. subtilis*, *E. coli* and *F. tularensis* capitalize on their rod shape to increase chemotaxis and enhance uptake for subsequent infectious continuation [13]. The low aspect ratio and condensed structure of rods increases motility by reducing inhibitory forces of fluid dynamics and allowing for rapid directional changes via tumbling [15,16]. These are only a few examples out of many that demonstrate the influences of morphology on the biological interactions of micro- and nano-scale structures.

Nanostructures, which can be broadly defined as materials exhibiting at least one dimension that is less than 1000 nm [17,18], have steadily garnered attention for applications within the biological sciences. Continued development of both synthetic and preparative techniques has led to the establishment of a multitude of nanostructures prepared from both organic and inorganic materials. Initially, nanostructures were applied therapeutically as carriers to enhance the circulation time of and decrease the degradation or undesired uptake of encapsulated or bound actives [19]. In doing so, these platforms attempted to evade the immune cell populations of the mononuclear phagocyte system (MPS), which are phagocytic cells primarily within the liver, spleen, lung, lymph nodes and kidneys that often remove these nanocarriers before achieving their objective. But, research efforts to develop immunomodulatory treatments, geared toward eliciting controlled inflammatory or tolerogenic responses, have shifted the focus to rationally designing nanostructures for uptake by specific immune cell subsets, namely professional antigen-presenting cells (APCs) that primarily include dendritic cells, macrophages and B cells. These broadly defined cell types are composed of dozens of subsets that each possess unique functions, having evolved to remove and respond to the diversity of micro and nanostructures characteristic of infectious agents. Furthermore, *in vivo* generated nanovesicles (i.e., exosomes) have been identified as a means of cellular communication employed by APCs and a variety of other cell types [20], presenting a system often hijacked by immunosuppressive and metastatic tumors [21,22]. APCs are central to the activation of effector and memory cells, like T cells, during immune responses and their diverse roles and mechanisms have been reviewed frequently [23–25]. The targeting of these specific subsets of APCs for improved control over and reproducibility of elicited immune responses remains a key objective and challenge for immunotherapy and vaccination.

To meet this central objective of minimizing nonspecific uptake by the MPS and enhancing APC subset targeting, researchers employing nanocarriers must carefully select both the characteristics of the base material as well as the nanoscale features of their vehicle. It is well established that a variety of physicochemical characteristics, such as surface charge, size, shape and surface chemistry, play a role in how the nanobiointerface is defined and how the nanostructure interacts with surrounding biological system [26]. As such, a number of reviews have been written to explore how a single characteristic, such as size [27] or chemistry [28], influences nanomaterial interactions. But in addition to these material properties, the nanostructure morphology has emerged as an equally important feature of nanocarriers that can dictate mechanisms of endocytosis, biodistribution and degree of cytotoxicity. In this review, we will highlight how the morphological features of nanostructures can be used to tailor their effectiveness during therapeutic immunomodulation. Features associated with a variety of nanoparticle morphologies will be highlighted for their effect in defining biodistribution and cellular uptake, eliciting an immunological response, permitting ligand attachment and presentation, achieving sustained release and enhancing theranostic strategies.

### Inherent features of nanoparticle morphologies

Morphological features of nanostructure-like shape and aspect ratio play a vital role in determining circulation time, biodistribution, toxicity, cellular uptake and therapeutic efficacy [29]. The vast majority of nanocarriers used in the transport of therapeutics are spherical in shape, and thus categories of nanostructures can be broadly divided between spherical or non-spherical (Figure 1). Spherical nanocarriers range from micellar to vesicular, which includes hollow, solid core and bicontinuous internal structures. Common nonspherical structures include rods, discs, cylindrical or worm-like micelles (filomicelles), wires and sheets. Many of these nanostructure morphologies have been assessed for therapeutic delivery with and without modifying their surface chemistries or incorporating targeting moieties, and it has become apparent that morphology alone can have a significant impact on efficacy and utility for specific applications. In part due to evolutionarily driven adaptations resulting from interactions with viral pathogens, nanocarriers have emerged as advantageous vehicles for interacting with cells and organs of the immune system. Here, we discuss how morphology-dependent aspects of nanocarriers impact biodistribution and cellular interactions with respect to immunotherapy.

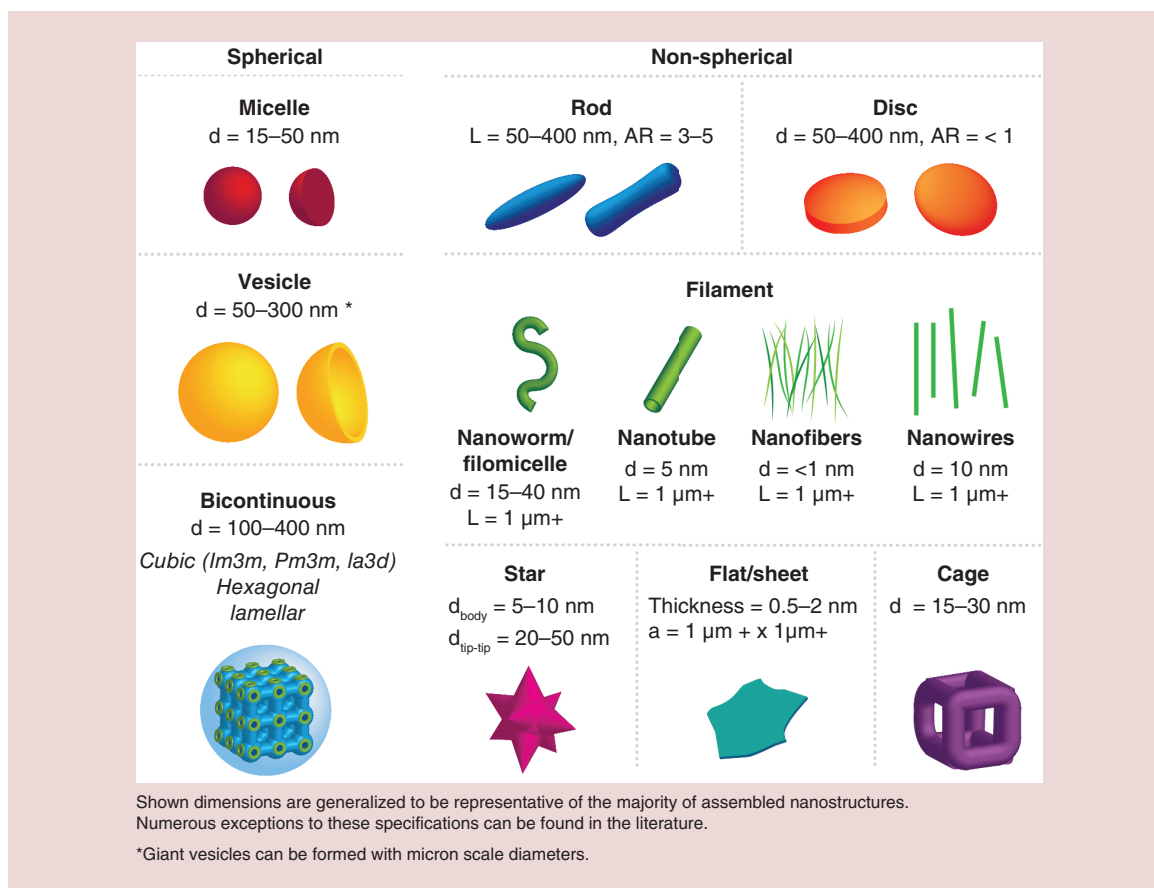


**Figure 1. Schematics of the general structural classifications of nanomaterial morphologies discussed in this review, separated into spherical and nonspherical categories.**

a: Area; AR: Aspect ratio; d: Diameter; L: Length.

### Circulation, biodistribution & toxicity

Circulation time is an important factor in determining the biodistribution and cellular uptake of nanocarriers and is often a critical parameter in their design. As such, nanostructure morphology has been shown to strongly impact the circulation time and resulting biodistribution of self-assembled polymeric nanocarriers. For example, Yi *et al.* studied the ability of various nanostructure morphologies composed of poly(ethylene glycol)-*bl*-poly(propylene sulfide) (PEG-*bl*-PPS) block copolymer to associate with diverse inflammatory cells in a mouse model of atherosclerosis. To better assess the influence of morphology, micelles ( $\sim 20\text{ nm}$ ), vesicular polymersomes ( $\sim 100\text{ nm}$ ) and high aspect ratio filomicelles ( $1\text{ }\mu\text{m}$  length) were each fabricated to possess the same surface chemistry and loaded with near infrared fluorescent agent indocyanine green (ICG) for organ-level tracking [30]. Mice injected intravenously with the ICG-loaded nanostructures revealed a significantly longer circulation time for filomicelles as evidenced by minimal accumulation of ICG in multiple organs and continued detection in blood serum when compared with micelles and polymersomes. Similarly, Park *et al.* showed that the circulation times of elongated nanoworms were greater than for spherical nanostructures [31]. However, seminal work by Geng *et al.* reported that the circulation time of filomicelles is highly dependent on length, where shorter filomicelles were cleared more quickly from the circulation compared with their longer counterparts [32].

In the case of inorganic nanomaterials, Talamini *et al.* tested gold nanostructures with different size and shape for their anatomical distribution [33]. Spherical gold nanostructures with  $50\text{ nm}$  diameters showed greater retention in organs compared with their  $10\text{ nm}$  diameter counterparts, which is credited to the higher internalization ability of larger particles in cells and efficient escape of smaller particles via endothelial cells. In the same study, gold nanorods showed lower penetration ability in organs and rapid clearance compared with the spherical nanoarchitectures, while star-like nanostructures showed rapid penetration through lung parenchyma thereby accumulating higher

amounts in lungs (Figure 2). Huang *et al.* further reported that the organ biodistribution and clearance of rod-shaped structures was also dependent on their length [34]. This study showed rapid clearance of 240 nm mesoporous silica nanorods and superior distribution of short nanorods in the liver, whereas 450 nm nanorods were distributed in the spleen. The biodistribution of bicontinuous structures such as cubosomes and hexosomes has been recently documented by Tran *et al.* In this study, lipid-based cubosomes showed more rapid accumulation in the liver post intravenous injection compared with hexosomes, however, both structures favored accumulation in the liver and spleen [35].

Some reports suggest that toxicity of nanostructures is morphology-dependent [33]. For example, Yu *et al.* investigated acute toxicity of silica nanostructures with varied geometry and porosity post intravenous injection [36]. In this study, mesoporous silica nanostructures showed greater toxicity due to vascular damage compared with the nonporous silica nanostructures. Specifically, mesoporous silica nanorods with long aspect ratio reported to show lower maximum tolerated dose than nanorods with short aspect ratio, which is attributed to the greater silica protein interaction. Investigations of carbon nanotubes have uncovered the concept of frustrated phagocytosis in a mechanism similar to asbestos pathogenicity, where macrophages are unable to engulf high aspect ratio particles with lengths greater than 15–20  $\mu\text{m}$  [37]. The resulting phagocytic burst produces pro-inflammatory cytokines and reactive oxygen species (ROS) that cause significant toxicity. In a study by Boyles *et al.* systematic investigation of multi-walled carbon nanotubes revealed that these harmful effects were dependent on the fiber length while crystallinity and metal content had little influence [38]. When engineering nanoparticle constructs, it is essential to consider immune responses in the context of topological properties inherent in unique structural morphologies.

### Cellular uptake

Morphology can determine the physical properties of nanostructures, such as shape, size and stiffness, which can strongly influence specific and nonspecific cellular uptake and internalization [39]. Barua *et al.* reported higher nonspecific cellular uptake of polystyrene-based nanospheres by breast cancer cells (BT-474, SK-BR-3 and MDA-MB-231) compared with their nano-rod and disc counterparts [40]. However, higher cell specific uptake of nanorods than spheres and discs was found after coating them with monoclonal antibody, trastuzumab. This was credited to the higher surface area per unit volume of nanorods that led to higher adsorption of trastuzumab. Furthermore, researchers have also reported role of stiffness for rod and spherical structures in cellular internalization. Garapaty *et al.* documented an inverse relation between stiffness and cellular internalization for rod-shaped polystyrene-based systems [41]. However, spherical particles showed no effect in cellular internalization upon change in stiffness.

On the other hand, cellular uptake of nanostructures has been reported to be cell type-specific. Agarwal *et al.* reported that mammalian epithelial cells and immune cells prefer disc-shaped nanostructures with high aspect ratio (2–3) compared with lower aspect ratio ( $\sim 1$ ) discs and nanorods [42]. In the same study, researchers demonstrated the relationship between shape and the mechanism of uptake. Epithelial cells were shown to internalize nanodiscs by a caveolae-mediated pathway and nano-rods and spheres by macropinocytosis. Similarly, Aldossari *et al.* reported superior activation and degranulation of mast cells by silver nanowires compared with spherical silver particles [43]. The cellular uptake of nanostructures in various organs is shape dependent and cell-type specific *in vivo*. The aforementioned work by Yi *et al.* demonstrated preferential uptake of nanostructures with different morphologies post intravenous injection into mice [30]. In this study, cylindrical micelles (filomicelles) displayed higher uptake by monocytes, granulocytes, neutrophils and macrophages in the blood compared with spherical nanostructures such as polymersomes and micelles. Conversely, spherical nanostructures outperformed filomicelles in associating with immune cells in the spleens and liver. Despite the evidence of geometrical features of nanostructure affecting cellular uptake, one should be careful not to overly generalize. This process is dependent on the adsorbed protein corona composition and structure, which will vary depending on the specific surface properties of the nanomaterial utilized as well as the blood composition and disease state.

### Immune cell interactions & induction of immune responses

Induction of cellular and/or humoral responses is prerequisite for successful immunization. Nanostructures have been key components of vaccine formulations long before their role in enhanced APC targeting was known, with alum particulates, virus-like particles and diverse oil-based nanoemulsions of bacterial and viral components being employed for hundreds of years [44]. Preferential targeting of immune cells for the purposes of targeted vaccination using various nanostructure morphologies has been documented. For instance, Dowling *et al.* investigated different PEG-*bl*-PPS polymer-based nanostructure morphologies and their role in targeting immune cells [45]. This study

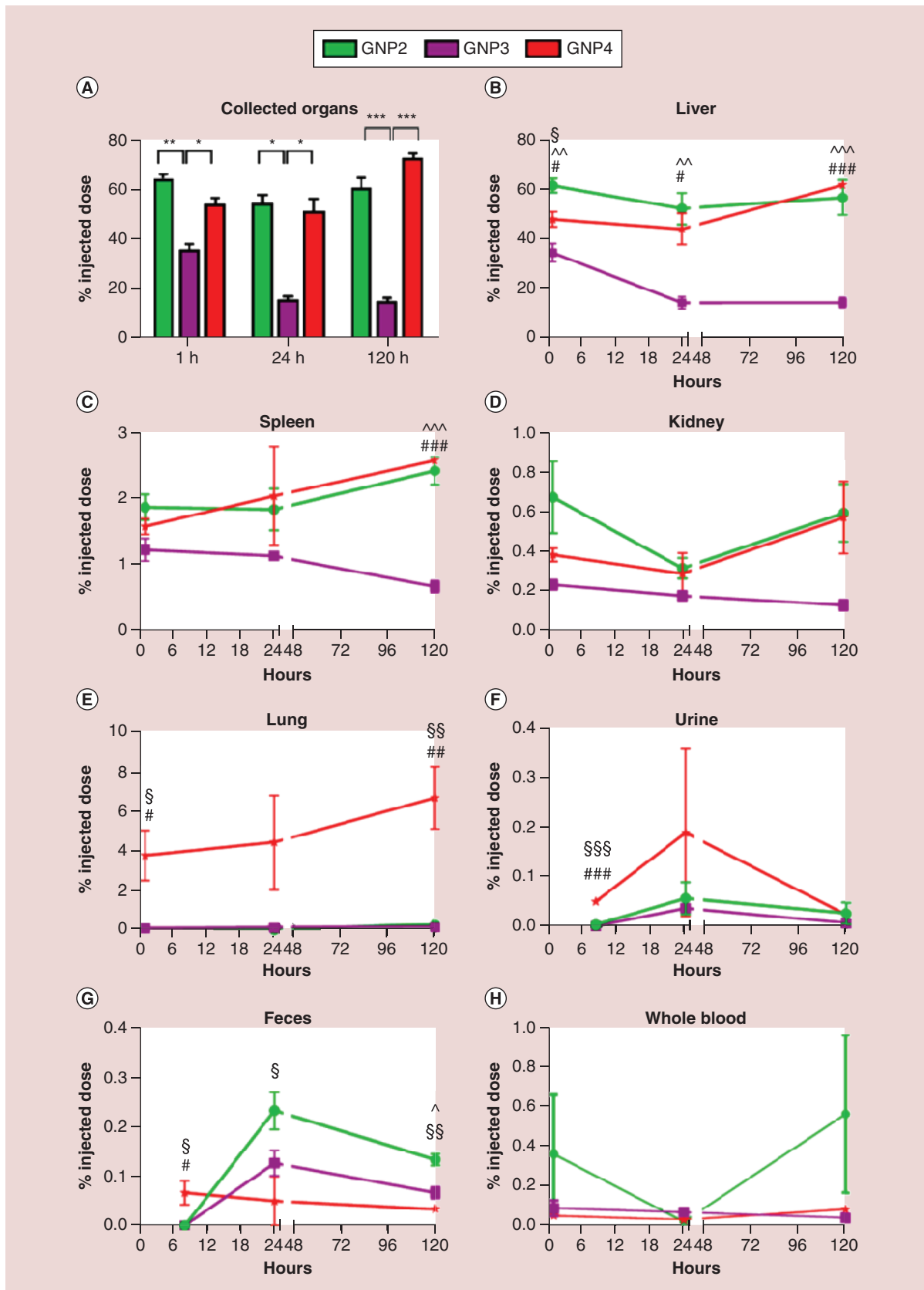


**Figure 2.** Inductively coupled plasma mass spectrometry analysis of gold from spherical (GNP2), rod (GNP3) and star-shaped (GNP4) AuNPs show morphology-dependent uptake over 120 h in treated mice. Presented as the fraction of injected dose, significant differences between shapes were found (A) overall, (B–E) by organ, (F–G) route of excretion and (H) circulation. Statistical significance is represented as (^) for spheres/rods, (§) for spheres/stars and (#) for rods/stars ( $p < *0.05$ ,  $**0.005$ ,  $***0.0005$ ). Reprinted with permission from [33] © ACS Publications (2017).

showed that 120 nm vesicular polymersomes preferentially associated with dendritic cells following subcutaneous injection *in vivo* when compared with 30 nm spherical micelles and 50 nm filomicelles. Polymersomes loaded with TLR8 agonist CL075 showed neonatal DC maturation and favored Th1 immunity in newborn mice. Recently, Yamazaki *et al.* examined different poly(sarcosine)-block-poly(L-lactic acid) morphologies carrying tumor-associated carbohydrate antigen Lewis y ( $Le^y$ ) to target B cells in T-cell deficient mice to enhance antibody responses [46]. This report showed that post intraperitoneal injection of nano-sheets comprised of interdigitate monolayer structures interact efficiently with B cells and induced greater Anti- $Le^y$  antibodies compared with nano-sheets with vesicle and rod-shaped morphologies. Kumar *et al.* studied size and shape dependent modulation of immune responses using polystyrene-based nanostructures [47]. Polystyrene nanospheres carrying ovalbumin (OVA) as a model antigen promoted a Th1 response whereas rod-shaped structures induced a higher Th2 response. The same study also showed that the smaller spherical particles (~193 nm) induced both Th1 and Th2 responses as compared with larger spherical particles (~521 nm). In another study, Dykman *et al.* reported that gold nanospheres conjugated with BSA and CpG generated greater antibody responses than their nano-star, rod and shell counterparts [48].

In addition to applications for vaccination, nanostructure morphology has demonstrated several advantages for immunotherapeutic and theranostic (combined delivery of therapeutics and diagnostics) strategies. Alaarg *et al.* showed that micelles carrying simvastatin decreased macrophage burden in atherosclerotic plaques, thereby reducing vessel wall inflammation when compared with simvastatin-loaded vesicular liposomes. This result was credited to higher cellular targeting of micelles to plaque macrophages [49], which was consistent with the previously discussed investigation by Yi *et al.* that compared vesicular versus micellar nanostructure cellular biodistributions in an atherosclerotic mouse model [30]. In another study, Tian *et al.* assessed polypyrrole composite particles with different morphologies as a multimodal immune-theranostic and therapeutic platform for cancer [50]. Raspberry-shaped polypyrrole particles containing Fe elements ( $Fe^{2+}$  and  $Fe^{3+}$ ) were found to outperform spherical and gibbous-shaped counterparts and showed enhanced photothermal killing of cancer cells while simultaneously tracking tumor size with magnetic resonance imaging. Furthermore, these particles showed morphology-dependent maturation and migration of a large number of dendritic cells into lymph nodes *in vivo*, which is a critical step in developing cytotoxic responses against cancer. Du *et al.* developed an oxidation-responsive perylene bisimide end-capped PEG-bi-PPS (PEG-PPS-PBI) immunotheranostic vesicular polymersomes, which allowed fluorescence-based detection of immune cell populations upon intracellular oxidation of the PPS unit [51]. Oxidation-induced disassembly of the tetrablock copolymer vesicles within cell endosomes resulted in disruption of the  $\pi$ - $\pi$  stacking of PBI to shift the fluorescence emission from 640 to 550 nm and mark cells that received intracellular payloads. Using this method, payload delivery could be traced via 550 nm emissions to various APC subsets, while false positives from simple membrane association could be assigned to NK cells displaying 640 nm emissions. In contrast to the red emission of the PEG-PPS-PBI-PPS-PEG vesicles, PEG-PPS-PBI-PPS-PEG micelle fluorescence was not detectable due to quenching effects, suggesting morphology-dependent differences in  $\pi$ - $\pi$  stacking densities within hydrophobic cores. Development of these type of platforms could be beneficial to more accurately identify targeted cells during immunotherapy and improve mechanistic understandings of the sources of elicited immune responses to improve reproducibility.

Due to their general biocompatibility, bioresorptive capacity and their potential to be tailored to meet specific structural and functional criteria, peptide amphiphiles are being designed and applied toward the treatment of a host of immunological diseases [52]. One specific application they have found to be particularly useful is in the development of novel subunit vaccines. Peptide nanofibers have shown to be self-adjuncting, or capable of enhancing the immunogenicity of subunit antigens. As such, their incorporation into vaccines can often alleviate the need for adding more potent adjuvants, such as toll-like receptors, that are associated with increased reactogenicity [53]. Originally ascribed to solely the specific peptide sequence, more evidence is emerging to indicate that this self-adjuncting effect is conferred by the self-assembled nanofibrillar structure [54].

The self-adjuncting effect of peptide nanofibers has been described in a number of recent publications. Chen *et al.* described the attachment of a short peptide domain (QQKFQFQFEQQ), Q11, to a model peptide antigen from ovalbumin, OVA<sub>323-339</sub>, to prepare antigen-bearing peptide nanofibers [53]. The peptide nanofiber vaccine elicited a high-titer and high-affinity IgG response. The induced response was CD4 T cell dependent and lacked the local inflammatory response often observed with alum-based adjuvants. This lack of injection site inflammation was attributed to the vaccine's restricted activation of dendritic cells rather than a combination of both dendritic cells and macrophages. Chesson *et al.* similarly demonstrated this characteristic when eliciting a CD8 T cell response [55]. The authors prepared Q11 nanofibers displaying the H-2k<sup>b</sup>-restricted OT-I peptide epitope and demonstrated that

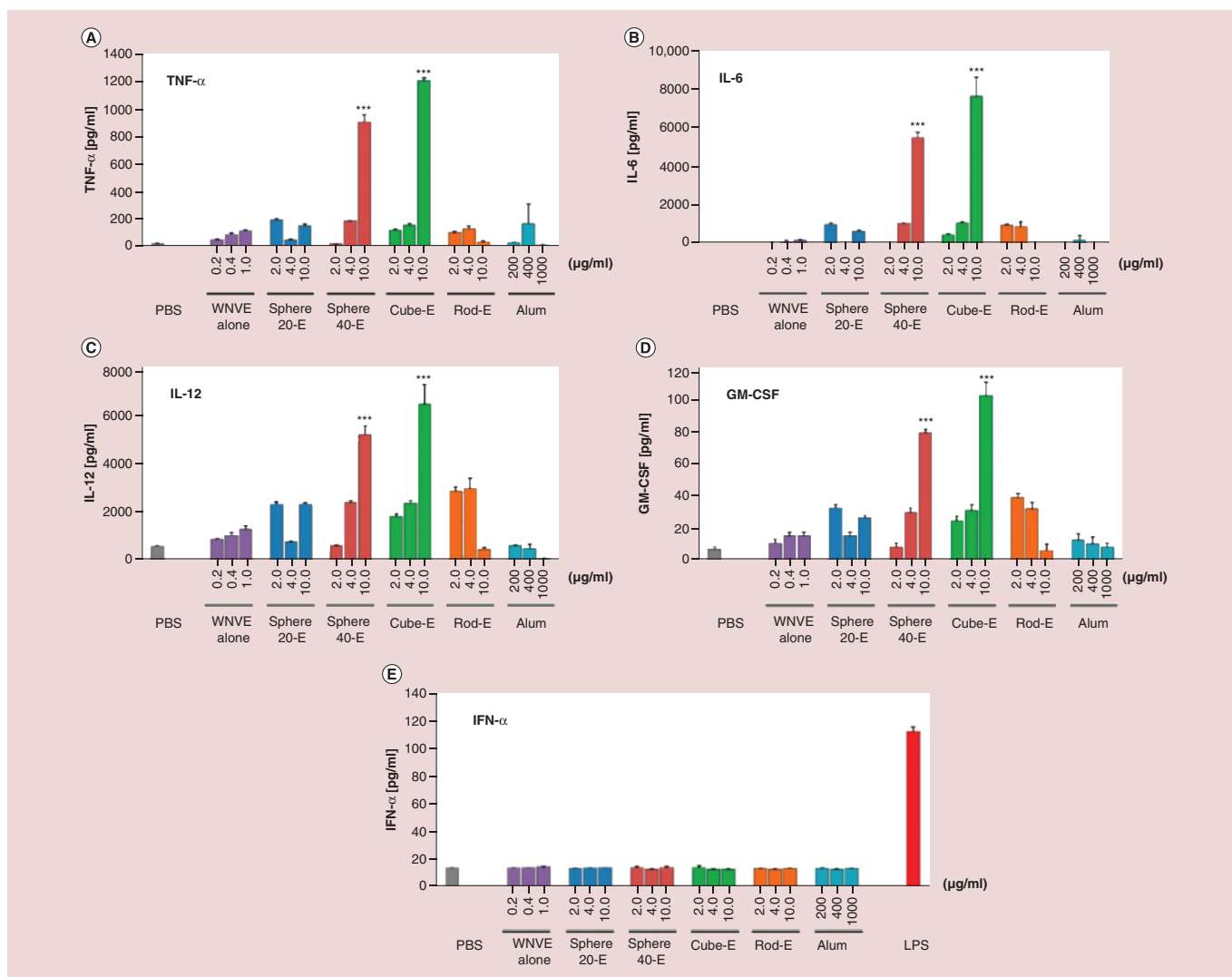


**Figure 3. Nanosphere and nanocube morphologies retained in lysosomes elicit a stronger antibody response through the increased release of proinflammatory cytokines.** Production of (A) TNF- $\alpha$ , (B) IL-6, (C) IL-12 and (D) GM-CSF in BMDCs was found to be significantly higher with 10  $\mu\text{g/ml}$  of spherical and cubic nanoparticles compared with free drug, smaller spheres, rods, alum and PBS. (E) No difference was found in lower doses, or in IFN- $\alpha$  production among the groups. Statistical significance is represented by \*\*\* $p < 0.001$ . BMDC: Bone marrow-derived dendritic cell; LPS: Lipopolysaccharide; PBS: Phosphate buffered saline.. Reprinted with permission from [56] © ACS Publications (2013).

the self-adjuncting peptide nanofibers were capable of evoking both a robust effector and recall CD8<sup>+</sup> T cell response. This ability to be applied as adjuvant systems for both CD4 and CD8 T cell responses has garnered significant interest for designing, incorporating and utilizing peptide nanofibers in scaffold-based vaccines.

Although several reports show morphology-dependent interactions of nanostructures with immune cells and induction of enhanced immune responses, the exact mechanisms involved in this process remain unclear. Unfortunately, few studies have further investigated the underlying intracellular and biochemical mechanisms behind these morphology-dependent responses to nanocarriers. Niikura *et al.* did present a more mechanistic investigation into this process for their nanostructures. They documented immune modulation and antibody production against West Nile Virus using gold nanostructures with sphere, cube and rod morphologies [56]. This study demonstrated that nanorods escaped from the lysosome to the cytosol to activate NLRP3 inflammasome and generate antibody responses. In contrast, nano-spheres and cubes were retained in the lysosome and induced secretion of high levels of pro-inflammatory cytokines, TNF- $\alpha$ , IL-6, IL-12 and GM-CSF, that induced even greater antibody responses (Figure 3). Rudra *et al.* has sought to elucidate the specific mechanism through which peptide nanofibers exhibit

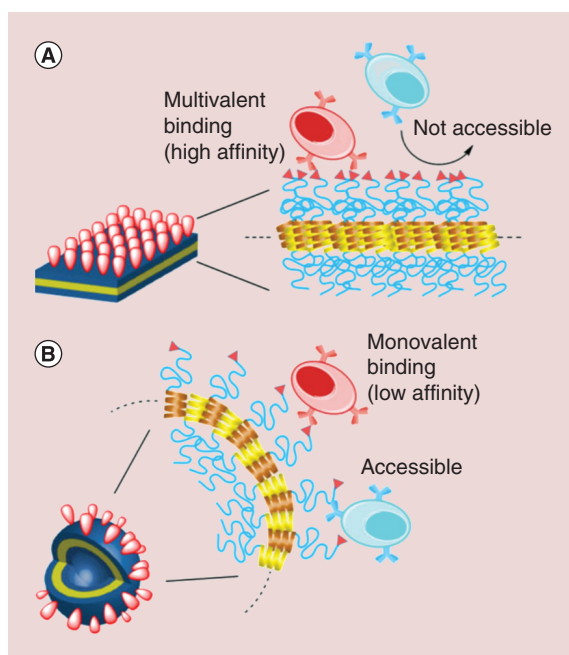


**Figure 4. Engineering of nanoparticle curvature determines the type and strength of immune cell binding.** Densely-packed ligands on a flat particle surface (A) allow for high affinity binding with multiple attachment points but inhibit access to deeper epitopes. Conversely, the loose packing found on highly curved particles (B) allows for deep penetration of immune cells but weaker binding due to the space between ligands. Reprinted with permission from [46] © Wiley (2016).

this immunostimulatory effect on APCs, dendritic cells and macrophages [57,58]. They conclude that autophagy plays a central role in the adjuvant mechanism of these supramolecular structures and highlight that future studies should focus on how adjusting physicochemical properties of the fibers (size, shape, stability) will alter their adjuvant properties. Overall, rational engineering of nanostructure morphologies for immunotherapeutic and theranostic strategies must take into account preferential uptake by distinct immune cell subsets as well as unique mechanisms of cellular stimulation that are in need of further study.

### Ligand interactions

The surface density and ligand–target affinity of targeting moieties displayed on the surfaces of nanocarriers strongly influence cellular uptake and specificity [26,59]. Indeed, biophysical analyses have demonstrated that nanocarrier size and shape can be optimized to enhance cellular interactions and internalization by endocytosis [26]. In this section, we discuss how the outer morphology of nanocarriers can affect interactions with cargo, targeting moieties, immunomodulatory ligands and access to the external environment before and during cellular uptake.

The characteristics of particle decoration are greatly affected by features of surface geometry. The aspect ratio, surface area and organization impact ligand density, orientation and conformation, which can all influence the efficacy and mechanism of cellular uptake. For example, Cherukula *et al.* took advantage of the large surface area of crystalline graphene quantum dots to maximize dihydrochloride histamine loading in the context of *in vitro* leukemia-induced immunosuppression (K-562 cells) [60]. This construct was able to successfully scavenge and inhibit further production of ROS, which are known to inhibit NK and T cell targeting of cancer cells. Han *et al.* found success using MoS<sub>2</sub> nanosheets protected by PEG and functionalized by CpG ligands [61]. With a sheet size of 500 nm and a thickness of 2 nm, these constructs are considered 2D structures, thereby maximizing the surface area and ligand packing for the given substrate mass [62]. Delivery of CpG loaded MoS<sub>2</sub> nanosheets resulted in increased levels of CD80, CD86, TNF- $\alpha$  and IL-6 with minimal toxicity in DC2.4 and RAW 264.7 cultures, indicating effective dendritic cell maturation and pro-inflammatory responses. When incubated with 4T1 breast cancer cells, MoS<sub>2</sub> sheets significantly reduced proliferation and increased cytotoxicity through anti-tumor cytokines. Utilizing the known tumor suppressing [63] photothermal functionality of MoS<sub>2</sub> to absorb near infrared irradiation, CpG uptake and immune stimulation were further increased *in vitro*.

A variety of studies have explored the effect of ligand density on the immune response to stimulants and antigens with a range of conclusions [64]. Ferritin nanocages induced ligand clustering based on the orientation of the edges, which synergistically increased the avidity of cancer neoantigens to induce robust amplification of targeted T cells in immunocompetent mice [65]. These findings may be explained by Yamazaki's work investigating the *in vivo*



presentation of tumor-associated antigens on organic polymer spheres, sheets, tubes and vesicles with a range of nanoparticle curvature [46]. The antigenicity of the decorated constructs showed an interesting trend in immune response that closely followed a model of physical spacing. Particles with a higher degree of curvature were found to have an increase in IgM production against epitopes deeper within the structure, indicating that the increased spacing between ligands on a curved surface allows for better penetration of B cells at the expense of low affinity binding (Figure 4). Conversely, the more planar constructs were found to produce high levels of IgM against the ligand with highest surface density. Overall, Yamazaki and coworkers uncovered the ability of B cells to switch between two distinct modes of epitope recognition in mice based on the particle morphology and subsequent ligand density. As such, there is evidence to suggest that other types of immune cells have similar flexibility in response to foreign shapes and patterns that can be exploited in immunoengineered nanomaterials. Many studies [62,66] capitalize on a variety of morphology-dependent features to enhance vaccine delivery of proteins based on the natural protein corona formation when foreign materials are introduced to biological systems. The Li group utilized the high surface area of graphene oxide nanosheets to spontaneously adsorb OVA and lysozyme at a density high enough to maintain the natural protein conformation and stabilize hydrophobic moieties [67]. After *in vitro* administration, the planar surface of loaded sheets easily attached to dendritic cell membranes, increasing internalization, while the edges destabilized the membrane for endosomal escape. Overall, this nano-adjuvant system was able to elicit strong immune responses through increased production of effector cytokines and promotion of T cell cross-presentation.

Nanocarrier morphology can be engineered to optimize the conformation and display of simple small molecule targeting moieties or antigen fragments to enhance interactions with larger, more complex target ligands. Investigations by Witt found that rationally designed lipid bilayer discs were able to properly incorporate and display integral membrane antigens, conserving their conformation and promoting the development of antibodies toward multiple epitopes [68]. The immune response to this nano-vaccination construct was vastly superior to the more traditional detergent-solubilized protein antigens. A study by Ding *et al.* corroborated these findings through an enhanced response to controlled antigen orientation on their AuNPs *in vitro* [69]. These works demonstrate the need for a thorough understanding of protein structure and antigenic regions in order to rationally engineer nanocarriers morphologies that maintain biologically relevant conformations after administration. Kuai *et al.* designed lipid bilayer discs of synthetic HDL and ApoA1 to load CpG and display OVA *in vivo* [70]. The OVA/CpG lipid disc vaccine was administered to mouse models of xenograft B16/OVA melanomas, colon cancer and B16F10 melanoma. Compared with free OVA/CpG combinations, mice with this nanoconstruct showed 10–47-fold higher antigen-specific CTLs, fourfold higher tumor regression with anti-PD1, rejection of subsequent challenge and maintenance of protection after at least 2 months. The success of this vaccine is owed in part to the precisely engineered morphology of the bilayer nanodisc that effectively transported and presented immunostimulants in fully functioning biological systems.

Nanocarriers have also been utilized to contribute to the supramolecular structure of immunomodulatory constructs. The arrangement of morphological features on the particle surface can stabilize, connect, or serve as a diffusion barrier up to the macroscale. Recently, rationally engineered nanofibers were used to construct a protective scaffold for preconditioning pancreatic islet cells before transplantation. Using a blend of polycaprolactone (PCL) and poly(3-hydroxybutyrate-co-3-hydroxyvalerate) (PHBV) to ensure the highest viability, Bowers *et al.* fabricated a macroscale membrane of nanofiber sheets saturated with the immunomodulatory FTY720 to surround the islets and slowly elute doses in the therapeutic range for angiogenesis [71]. The exceptionally high local concentration of FTY720 near the construct was shown to reduce inflammatory macrophages and cytokines *in vivo* without detrimental effects to the surrounding tissue. In this way, the nanofiber morphology makes a significant contribution to the loading, swelling properties and structural support of a system expected to prevent hypoxic damage, impaired function and complete graft rejection.

### Sustained release

Nanostructures have ever more frequently been successfully utilized as central components within sustained delivery systems. Though not every morphology has been adapted for this purpose, two structures, namely cylindrical nanofibers and bicontinuous nanostructures, have exhibited characteristics that make them adept for this purpose. Each of these morphologies exhibit characteristics related to their nanostructure that enhance their potential for incorporation into sustained delivery systems for immunotherapy. Due to the potential for crosslinking nanofibers into porous gels and the internal channels of BCNs, both of these structures are capable of forming depots that permit the sustained release of an active from the site of administration.

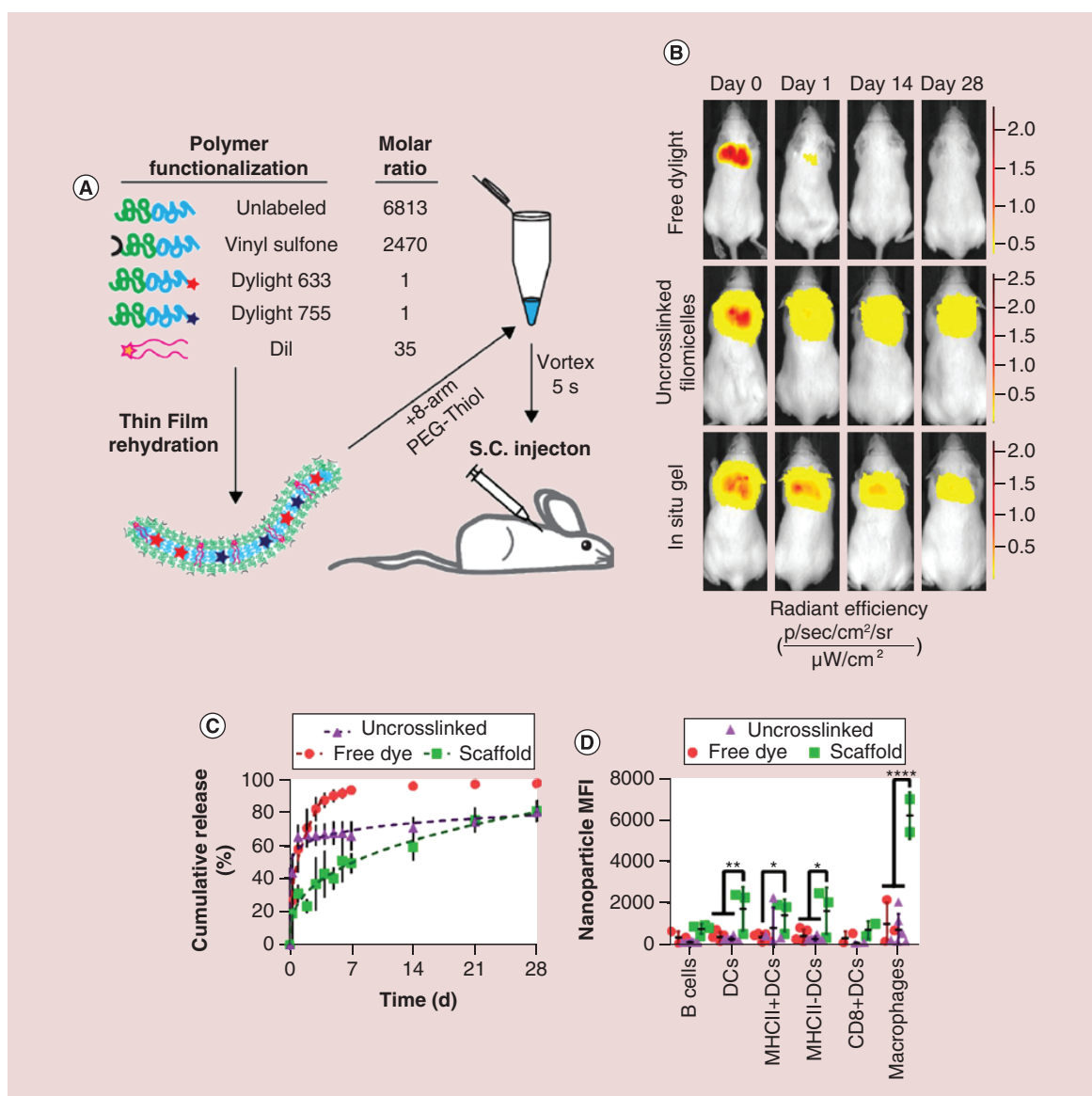


**Figure 5. Poly(ethylene glycol)-bl-poly(propylene sulfide) filomicelle-based scaffolds permit the sustained delivery of micellar delivery vehicles for immune cell uptake. (A)** Schematic depicting the individual components comprising the modular filomicelles. **(B)** Intravital fluorescence images comparing the release of free DyLight-755, uncrosslinked filomicelles and the *in situ* crosslinked filomicelle scaffold over the course of 1 month. **(C)** Cumulative release curves of the aforementioned groups representative of the loss of polymer from the injection site. **(D)** Flow cytometric analysis of micelle uptake within phagocytic immune cell populations within the draining lymph nodes of mice receiving either free DyLight, uncrosslinked filomicelles or the *in situ* crosslinked filomicelle scaffold 1 month post injection. Reprinted under the terms of the Creative Commons CC BY license [73] © Springer Nature (2018).

Relying on physical interactions, peptide-based nanofibers can be coalesced into hydrogel scaffolds or matrices for use in single-dose vaccine systems. Yang *et al.* who previously demonstrated the adjuvant effect of nanofibers prepared from D-peptide Nap-G<sup>DFDY</sup>, prepared both cationic and anionic D-peptide nanofibers through the introduction of either a lysine or glutamic acid residue [72]. These charged nanofibers were capable of forming supramolecular hydrogels when mixed in the presence of antigen. While all nanofiber-incorporating formulations were capable of eliciting an effective immune response following subcutaneous injection *in vivo*, the positively charged nanofibers elicited the strongest humoral response. The authors postulated that the nanofiber-based formulations outperformed the alum-based control due to their ability to more effectively control the release of antigen. Furthermore, the formulation incorporating positively charged nanofibers elicited a long-lasting antibody

Table 1. Summary of morphology-dependent immune responses elicited by different nanostructures.

| Morphology                    | Material         | Evaluated aspect   | Ref. |
|-------------------------------|------------------|--|------|
| Cage                          | Ferritin         | T cell amplification                                       | [65] |
| Cubosome                      | Phy-F127         | Payload, sustained release, cross-presentation             | [76] |
| Cubosome                      | PEG-PPS          | Release, DC activation                                     | [77] |
| Cubosome, hexosome            | Lipid            | Biodistribution  | [35] |
| Discoidal                     | HDL              | Antigen-specific production, tumor regression/survival     | [70] |
| Discoidal, rod                | Polystyrene      | Specific and non-specific binding                          | [40] |
| Discoidal, rod                | PEGDA            | Uptake   | [42] |
| Discoidal, spherical          | HDL              | Clearance, targeting; atherosclerosis                      | [48] |
| Discoidal, spherical          | Lipid + MSP      | Stability, epitope masking                                 | [68] |
| Filamentous                   | PEG-PPS          | Biodistribution  | [30] |
| Filamentous                   | Iron oxide       | Targeting  | [31] |
| Filamentous                   | PHBV-PCL         | Drug-eluting, physical barrier; islet cell transplants     | [53] |
| Filamentous                   | Peptides         | uptake, differentiation, cross-reactivity                  | [55] |
| Filamentous                   | Peptides         | APC uptake, adjuvanticity                                  | [58] |
| Filamentous                   | Peptides         | CD8 T cell stimulation without adjuvant                    | [71] |
| Filamentous gel               | Peptides         | T cell response, tumor growth                              | [52] |
| Filamentous gel               | Peptides         | CD8 T cell activation, proliferation                       | [54] |
| Filamentous gel               | PGA-chitosan     | Antigen specific cross-presentation, titers, adjuvanticity | [72] |
| Filamentous gel, spherical    | PEG-PPS          | Morphology transition, release                             | [73] |
| Filamentous scaffold          | Peptides         | CD8 T cell, memory, effector response                      | [57] |
| Filamentous, flat             | pSarc-LLAIB      | IgM production, growth inhibition, ligand density          | [46] |
| Filamentous, flat, spherical  | Silver           | Uptake; mast cell degranulation                            | [43] |
| Filamentous, spherical        | PEG-PEE; PEG-PCL | Uptake, circulation  | [32] |
| Filamentous, spherical        | PEG-PPS          | Biodistribution; lymph nodes, spleen                       | [45] |
| Flat                          | MoS <sub>2</sub> | Payload uptake, stimulation                                | [61] |
| Flat                          | Graphene oxide   | Antigen display, uptake, endosomal escape                  | [67] |
| Raspberry, gibbous, spherical | Polypyrrole      | Targeting, MRI visualization                               | [50] |
| Rod                           | Silica           | Biodistribution, excretion                                 | [34] |
| Rod, cubic, spherical         | Gold             | Uptake, antibody production, adjuvanticity                 | [56] |
| Rod, spherical                | Silica           | Renal excretion  | [36] |
| Rod, spherical                | PAA, PVP, PEI    | Uptake, antibody titers                                    | [41] |
| Rod, spherical                | Polystyrene      | Th1 and Th2 response                                       | [47] |
| Rod, star, spherical          | Gold             | Biodistribution, excretion                                 | [33] |
| Spherical                     | PEG-PPS          | Targeting  | [51] |
| Spherical                     | Graphene         | Loading, release   | [60] |
| Spherical                     | Polystyrene      | Antibody production  | [64] |
| Spherical                     | Gold             | APC uptake, Th1 and Th2 response                           | [69] |

HDL: High-density lipoprotein; LLAIB: L-Leu-Aib; MSP: Membrane scaffold protein; PAA: Poly(acrylic acid); PEG-PPS: Poly(ethylene glycol)-poly(propylene sulfide); PEG-PEE: Poly(ethylene glycol)-poly(ethylene); PEG-PCL: Poly(ethylene glycol)-polycaprolactone; PEI: Poly(ethylenimine); PHBV-PCL: Poly(3-hydroxybutyrate-co-3-hydroxyvalerate)-polycaprolactone; PVP: Poly(vinylpyrrolidone).

response that failed to decline even after 28 weeks. This enhanced potency occurred due to an increase in antigen uptake by dendritic cells, which the authors attributed to the effect of the positive surface charge of the D-peptide nanofibers. In addition to their role in prophylactic vaccines, peptide nanofibers are also being applied in the development of therapeutic vaccines against tumors. Xing *et al.* prepared fibrous hydrogels from *N*-fluorenylmethoxycarbonyl diphenylalanine helical peptide nanofibers [52]. These nanofibers exhibit a negative surface charge, and the authors were able to stabilize and modulate the mechanical properties of the hydrogel through the addition of the positively charged poly-L-lysine. The helical nanofibers that compose the scaffold resemble the fimbrial antigen, and the authors exploited this similarity to promote T cell activation. When used to treat a murine tumor model, the peptide nanofiber scaffold, without the addition of exogenous antigen, immunostimulatory

agents or additional adjuvants, successfully elicited a T cell response that mitigated tumor growth. Peptide-based nanofibers have successfully been utilized in a variety of immune-related applications. The nanofibrillar morphology is well adapted for sustained delivery applications as it can be readily exploited to form a depot for either sustained delivery or sustained presentation.

In addition to the matrix or scaffold systems formed by peptide nanofibers, cylindrical polymer-based nanostructures have also been explored for the development of sustained delivery platforms. While similar to their peptide-based counterparts in that the length scale of the cylindrical morphology permits the formation of a depot through a combination of entanglements and physical or covalent interactions, the morphologic fluidity of polymer-based systems presents a unique design opportunity. Recently, Karabin *et al.* described how morphologic transitions within polymer systems could be exploited for sustained nanoparticle delivery [73]. In their work, the authors utilized the amphiphilic diblock copolymer PEG-*bl*-PPS for the self-assembly of cylindrical filomicelles. Surface functionalization of the filomicelles with vinyl sulfone groups permitted their cross-linking with thiol functionalized multi-arm PEG into a fibrous, hydrogel scaffold. The self-assembled morphology of block copolymers is dictated by the balance of hydrophilic and hydrophobic character within the system, which influences surface tension driven stabilization of nanostructures. Here, the authors exploited the oxidation sensitivity of PEG-*bl*-PPS to shift the overall hydrophilicity of the block copolymer both *in vitro* and *in vivo* to induce a shift from cylindrical to spherical structures, a process known as the cylinder-to-sphere transition [74,75]. As this morphologic transition occurred, the cylindrical structures that once served as the scaffold struts re-assembled into micellar vehicles for continuous delivery from the injection site. Intravital fluorescence imaging was used to confirm that release occurred over the course of 1 month and flow cytometric analysis demonstrated that the released micelles could reach immune cell populations in both the draining lymph nodes and spleen (Figure 5). Given the ability to achieve sustained nanocarrier release, this platform could serve as the basis for single-dose vaccine systems as well as for the immunomodulatory treatment of chronic immune dysregulation.

In addition to fibrillar and cylindrical nanostructures, bicontinuous nanostructures, such as cubosomes or polymeric bicontinuous nanospheres (BCNs), have also demonstrated a potential for their inclusion in the development of morphology-dependent sustained delivery systems aimed at modulating the immune system. These complex nanostructures can encapsulate a wide array of hydrophilic and lipophilic payloads due to their unique nanoarchitecture, which includes high internal surface area, extensive hydrophobic domains and an internal organization of separate nonintersecting aqueous channels. Rizwan *et al.* investigated how cubosomes, prepared with phytantriol and Pluronic F127, could be used to stimulate both cellular and humoral immune responses [76]. The submicron structures were loaded with a combination of TLR-agonists, monophosphoryl lipid A (MPL) and imiquimod, as well as the model antigen ovalbumin. The adjuvant loaded cubosomes were equally effective at generating humoral responses as the alum control, as comparable levels of ovalbumin-specific IgG antibodies were induced through both treatments. Furthermore, the authors observed significantly greater expansion of antigen-specific CD8<sup>+</sup> T cells in mice vaccinated with adjuvant-loaded cubosomes in comparison to both the adjuvant-loaded liposome and alum controls. The authors concluded that the cubosome's potential for sustained release translated into an enhanced capacity for inducing antigen-specific cellular responses.

Building off the extensive work in lipid based cubic systems, researchers have also begun to explore the use of block copolymers for the formation of polymeric BCNs. Comparable to their lipid-based counterparts with regards to extensive surface area and high loading potential for both hydrophilic and lipophilic actives, BCNs are advantageous due to the added stability provided by the high molecular weight polymers used in their formation. Bobbala *et al.* described the use of the PEG-*bl*-PPS block copolymer system for the scalable formation of BCNs [77]. In their work, the authors demonstrated the sustained release of both lipophilic and hydrophilic model molecules *in vitro*. To further demonstrate the potential application of these nanostructures in the development of subunit vaccines, the model protein antigen ovalbumin and TLR4 agonist MPL were co-encapsulated and applied in an *in vitro* bone marrow derived dendritic cell activation and antigen presentation assay.

## Conclusion

Due to the wide range of nanomaterials that have been developed and the sensitivity of the immune system to so many different physicochemical properties of nanoscale vehicles, it has proven difficult to extract general rules and mechanisms for the rational design of nanocarriers for immunotherapy. Some of the most insightful findings concerning the influence of morphology may come from studies that attempt to minimize variables by employing the same chemistries and source material for different structures. Despite the diversity of nanomaterials under

investigation, we have attempted to summarize key patterns that have emerged across numerous studies that link nanostructure morphology with elicited immune responses during immunotherapy (Table 1). Indeed, a variety of morphology-dependent parameters can provide multiple dimensions of function and control in targeting, cell uptake, loading efficiency, immune stimulation and sustained delivery of therapeutic and/or diagnostic agents. These results call for continued evaluation of the individual and integrated effects of nanocarrier morphology on immunomodulation and highlight the need for a better mechanistic understanding of the underlying biochemical and biophysical pathways of their action.

### Executive summary

#### Inherent features of nanoparticle morphologies

- Nanoparticle morphology independently affects circulation, biodistribution and cellular interactions.
- Polymeric filomicelles have shown longer circulation times *in vivo* compared with spherical particles of identical surface chemistry.
- While controlling for size, gold particles of rods, spheres and stars showed increasing ability to accumulate in tissue. Additionally, organ-specific distributions were found for rods of varying length and for bicontinuous nanostructures.
- Particles with high aspect ratios may induce cellular toxicity through frustrated phagocytosis as shown in early studies with carbon nanotubes.
- When combining the effects of multiple particle features, specific morphologies have a diverse range of effects that can act synergistically to promote or inhibit cellular uptake.
- The response to nanoparticle morphologies can be cell-type and disease specific, mediated in part by the mechanism of uptake, general function and local environment of each cell population.
- Spherical, filamentous, flat, rod and star-shaped particles showed preferential uptake into dendritic cells, macrophages and B cells. These differences can be utilized in producing specific Th1, Th2 or antibody responses for vaccinations, reduction of inflammation and cancer immunotherapy.
- The mechanisms of morphology-dependent cell interactions are in need of further investigation at the molecular level.

#### Ligand interactions

- Several studies have taken advantage of high surface area morphologies to maximize the effects of targeting and therapeutic surface decoration of nanoparticles.
- Nanoparticle structure directly impacts the surface density of conjugated ligands as a function of aspect ratio and curvature. Changes in ligand spacing has been shown to affect epitope presentation, immune cell penetration and the number of concurrent signals sent to a target cell.
- Lipid bilayer discs can be used to simulate complete cellular membranes in order to more accurately display protein antigens in correct conformations for immunostimulation.
- Nanofibers have been explored as integral structural components of supramolecular assemblies to modify local cellular environments.

#### Sustained release

- Hydrogels composed of crosslinked nanofibers serve as stable scaffolds for the slow release of loaded cargo with decreased local inflammatory responses.
- The cylinder-to-sphere transition of self-assembled filaments offers new thermodynamically driven mechanisms of controlled sustained release for immunomodulatory and diagnostic micelles.
- The complex internal architecture of bicontinuous nanostructures provides size- and molecular weight-dependent controlled release of therapeutics with advantages for intracellular delivery to and activation of antigen-presenting cell populations during vaccination.

### Future perspective

The work described here shows incredible potential for the controlled modulation and tuning of immune responses using nanoparticle shape and structure. We hope the exploration of diverse nanocarrier morphologies and their unique interactions with immune cells will continue, leading to a better understanding and rational use of complex and nonspherical structures. Morphology-based targeting presents an additional mechanism of achieving specificity by disproportionately modulating certain immune cell populations over others, which may prove particularly useful for avoiding nonspecific uptake by phagocytes of the MPS. External physical properties of nanocarriers greatly impact the bioavailability and cellular targeting of delivered payloads, while the internal architectures dictate loading capacity and release kinetics. Each of these individual features can be further enhanced and diversified in combination with mechanisms that can trigger changes in nanostructure morphology on-demand in responsive

to environmental conditions such as pH, temperature and ROS. These abilities will reduce the need for as well as supplement strategies employing nanoparticle surface engineering, which currently direct cell–nanoparticle interactions using surface charge, conjugated targeting ligands and minimization of adsorbed protein coronas. We envision nanostructure morphology becoming a key tool and essential criteria in the rational design of controlled delivery systems for immunomodulation and immunization.

#### Financial & competing interests disclosure

The authors have no relevant affiliations or financial involvement with any organization or entity with a financial interest in or financial conflict with the subject matter or materials discussed in the manuscript. This includes employment, consultancies, honoraria, stock ownership or options, expert testimony, grants or patents received or pending, or royalties. This work was supported by the National Science Foundation grant 1453576 and the National Institutes of Health Director's New Innovator Award no. 1DP2HL132390-01.

No writing assistance was utilized in the production of this manuscript.

#### References

Papers of special note have been highlighted as: ● of interest; ●● of considerable interest

1. Kaufman J, Völk H, Wallny HJ. A “minimal essential Mhc” and an “unrecognized Mhc”: two extremes in selection for polymorphism. *Immunol. Rev.* 143, 63–88 (1995).
2. Flajnik MF, Kasahara M. Origin and evolution of the adaptive immune system: genetic events and selective pressures. *Nat. Rev. Genet.* 11(1), 47–59 (2009).
3. Zimmerman LM, Vogel LA, Bowden RM. Understanding the vertebrate immune system: insights from the reptilian perspective. *J. Exp. Biol.* 213(5), 661–671 (2010).
4. Lina TT. Immune evasion strategies used by *Helicobacter pylori*. *WJG* 20(36), 12753 (2014).
5. Reddick LE, Alto NM. Bacteria fighting back: how pathogens target and subvert the host innate immune system. *Mol. Cell* 54(2), 321–328 (2014).
6. Marcos CM, de Oliveira HC, de Melo W de CMA *et al.* Anti-immune strategies of pathogenic fungi. *Front. Cell Infect. Microbiol.* 6(Pt 1), 142 (2016).
7. Hernando-Amado S, Blanco P, Alcalde-Rico M *et al.* Multidrug efflux pumps as main players in intrinsic and acquired resistance to antimicrobials. *Drug Resist. Updat.* 28, 13–27 (2016).
8. Moreno-Gamez S, Hill AL, Rosenbloom DIS, Petrov DA, Nowak MA, Pennings PS. Imperfect drug penetration leads to spatial monotherapy and rapid evolution of multidrug resistance. *Proc. Natl Acad. Sci. USA* 112(22), E2874–E2883 (2015).
9. Kuo H-Y, Chang K-C, Kuo J-W, Yueh H-W, Liou M-L. Imipenem: a potent inducer of multidrug resistance in *Acinetobacter baumannii*. *Int. J. Antimicrob. Agents.* 39(1), 33–38 (2012).
10. Tavanti A, Campa D, Bertozzi A *et al.* *Candida albicans* isolates with different genomic backgrounds display a differential response to macrophage infection. *Microbes Infect.* 8(3), 791–800 (2006).
11. Yemelin A, Brauchler A, Jacob S *et al.* Identification of factors involved in dimorphism and pathogenicity of *Zyoseptoria tritici*. *PLOS ONE* 12(8), e0183065 (2017).
12. Rossman JS, Leser GP, Lamb RA. Filamentous influenza virus enters cells via macropinocytosis. *J. Virol.* 86(20), 10950–10960 (2012).
13. Khandige S, Asferg CA, Rasmussen KJ *et al.* DamX controls reversible cell morphology switching in uropathogenic *Escherichia coli*. *mBio.* 7(4), e00642–16 (2016).
14. Prashar A, Bhatia S, Gigliozzi D *et al.* Filamentous morphology of bacteria delays the timing of phagosome morphogenesis in macrophages. *J. Cell Biol.* 203(6), 1081–1097 (2013).
15. Saragosti J, Silberzan P, Buguin A. Modeling *E. coli* tumbles by rotational diffusion. implications for chemotaxis. *PLOS One* 7(4), e35412 (2012).
16. Lushi E. Stability and dynamics of anisotropically tumbling chemotactic swimmers. *Phys. Rev. E.* 94(2–1), 022414 (2016).
17. Klaessig F, Marrapese M, Abe S. Current perspectives in nanotechnology terminology and nomenclature. In: *Nanotechnology Standards*. Murashov V, Howard J (Eds.). Springer New York, New York, NY, 21–52 (2011).
18. Buzea C, Pacheco II, Robbie K. Nanomaterials and nanoparticles: sources and toxicity. *Biointerphases.* 2(4), MR17–MR71 (2007).
19. Barenholz Y. Doxil<sup>®</sup> – the first FDA-approved nano-drug: lessons learned. *J. Control Release* 160(2), 117–134 (2012).
20. Lindenbergh MFS, Stoorvogel W. Antigen presentation by extracellular vesicles from professional antigen-presenting cells. *Annu. Rev. Immunol.* 36 435–459 (2018).
21. Rong L, Li R, Li S, Luo R. Immunosuppression of breast cancer cells mediated by transforming growth factor- $\beta$  in exosomes from cancer cells. *Oncol. Lett.* 11(1), 500–504 (2016).

22. Wu C-Y, Du S-L, Zhang J, Liang A-L, Liu Y-J. Exosomes and breast cancer: a comprehensive review of novel therapeutic strategies from diagnosis to treatment. *Cancer Gene Ther.* 24(1), 6–12 (2017).
23. Roche PA, Furuta K. The ins and outs of MHC class II-mediated antigen processing and presentation. *Nat. Rev. Immunol.* 15(4), 203–216 (2015).
24. Kashem SW, Haniffa M, Kaplan DH. Antigen-presenting cells in the skin. *Annu. Rev. Immunol.* 35, 469–499 (2017).
25. Jakubczik CV, Randolph GJ, Henson PM. Monocyte differentiation and antigen-presenting functions. *Nat. Rev. Immunol.* 17(6), 349–362 (2017).
26. Nel AE, Mädler L, Velegol D *et al.* Understanding biophysicochemical interactions at the nano–bio interface. *Nat. Mater.* 8(7), 543–557 (2009).
27. Shang L, Nienhaus K, Nienhaus GU. Engineered nanoparticles interacting with cells: size matters. *J. Nanobiotechnology* 12(1), 5 (2014).
28. Lane LA, Qian X, Smith AM, Nie S. Physical chemistry of nanomedicine: understanding the complex behaviors of nanoparticles in vivo. *Annu. Rev. Phys. Chem.* 66(1), 521–547 (2015).
29. Moghimi SM, Hunter AC, Andresen TL. Factors controlling nanoparticle pharmacokinetics: an integrated analysis and perspective. *Annu. Rev. Pharmacol. Toxicol.* 52, 481–503 (2012).
30. Yi S, Allen SD, Liu Y-G *et al.* Tailoring nanostructure morphology for enhanced targeting of dendritic cells in atherosclerosis. *ACS Nano* 10(12), 11290–11303 (2016).
- **This work directly compares the circulation time, organ distribution and immune cell uptake between spherical and filamentous nanoparticles in mice and demonstrates how these can change in a disease model of heart disease.**
31. Park J-H, Maltzahn von G, Zhang L *et al.* Systematic surface engineering of magnetic nanoworms for *in vivo* tumor targeting. *Small* 5(6), 694–700 (2009).
32. Geng Y, Dalhaimer P, Cai S *et al.* Shape effects of filaments versus spherical particles in flow and drug delivery. *Nature Nanotech.* 2(4), 249–255 (2007).
- **This seminal work is one of the first to demonstrate the benefit of high aspect ratio filomicelles for increasing circulation time by decreasing nonspecific cell uptake.**
33. Talamini L, Violatto MB, Cai Q *et al.* Influence of size and shape on the anatomical distribution of endotoxin-free gold nanoparticles. *ACS Nano* 11(6), 5519–5529 (2017).
- **This work shows morphology-dependent differences in circulation, organ uptake and route of excretion over time for gold nanoparticles shaped as spheres, stars and rods.**
34. Huang X, Teng X, Chen D, Tang F, He J. The effect of the shape of mesoporous silica nanoparticles on cellular uptake and cell function. *Biomaterial.* 31(3), 438–448 (2010).
35. Tran N, Bye N, Moffat BA *et al.* Dual-modality NIRF–MRI cubosomes and hexosomes: High throughput formulation and *in vivo* biodistribution. *Mater. Sci. Eng. C. Mater. Biol. Appl.* 71, 584–593 (2017).
36. Yu T, Greish K, McGill LD, Ray A, Ghandehari H. Influence of geometry, porosity, and surface characteristics of silica nanoparticles on acute toxicity: their vasculature effect and tolerance threshold. *ACS Nano.* 6(3), 2289–2301 (2012).
37. Murphy FA, Poland CA, Duffin R *et al.* Length-dependent retention of carbon nanotubes in the pleural space of mice initiates sustained inflammation and progressive fibrosis on the parietal pleura. *Am. J. Pathol.* 178(6), 2587–2600 (2011).
38. Boyles MSP, Young L, Brown DM *et al.* Multi-walled carbon nanotube induced frustrated phagocytosis, cytotoxicity and proinflammatory conditions in macrophages are length dependent and greater than that of asbestos. *Toxicol. In Vitro* 29(7), 1513–1528 (2015).
39. Gratton SEA, Ropp PA, Pohlhaus PD *et al.* The effect of particle design on cellular internalization pathways. *Proc. Natl Acad. Sci. USA* 105(33), 11613–11618 (2008).
40. Barua S, Yoo J-W, Kolhar P, Wakankar A, Gokarn YR, Mitragotri S. Particle shape enhances specificity of antibody-displaying nanoparticles. *Proc. Natl Acad. Sci. USA* 110(9), 3270–3275 (2013).
41. Garapaty A, Champion JA. Tunable particles alter macrophage uptake based on combinatorial effects of physical properties. *Bioeng. Transl. Med.* 2(1), 92–101 (2017).
42. Agarwal R, Singh V, Journey P, Shi L, Sreenivasan SV, Roy K. Mammalian cells preferentially internalize hydrogel nanodiscs over nanorods and use shape-specific uptake mechanisms. *Proc. Natl Acad. Sci. USA* 110(43), 17247–17252 (2013).
43. Aldossari AA, Shannahan JH, Podila R, Brown JM. Influence of physicochemical properties of silver nanoparticles on mast cell activation and degranulation. *Toxicol. In Vitro* 29(1), 195–203 (2015).
44. Irvine DJ, Hanson MC, Rakhra K, Tokatlian T. Synthetic nanoparticles for vaccines and immunotherapy. *Chem. Rev.* 115(19), 11109–11146 (2015).
45. Dowling DJ, Scott EA, Scheid A *et al.* Toll-like receptor 8 agonist nanoparticles mimic immunomodulating effects of the live BCG vaccine and enhance neonatal innate and adaptive immune responses. *J. Allergy Clin. Immunol.* 140(5), 1339–1350 (2017).

- **This work includes an exceptional display of the relative uptake rate of spherical and filamentous particles across immune cell populations in the lymph nodes and spleen, identifying exploitable differences for targeting and modulating specific immune responses.**
- 46. Yamazaki Y, Watabe N, Obata H, Hara E, Ohmae M, Kimura S. Immune activation with peptide assemblies carrying Lewis y tumor-associated carbohydrate antigen. *J. Pept. Sci.* 23(2), 189–197 (2016).
- 47. Kumar S, Anselmo AC, Banerjee A, Zakrewsky M, Mitragotri S. Shape and size-dependent immune response to antigen-carrying nanoparticles. *J. Control Release* 220(Pt A), 141–148 (2015).
- **This work examines the relationship between particle morphology and the resulting balance of Th1 and Th2 responses with all other factors held constant.**
- 48. Dykman LA, Staroverov SA, Fomin AS, Khanadeev VA, Khlebtsov BN, Bogatyrev VA. Gold nanoparticles as an adjuvant: Influence of size, shape, and technique of combination with CpG on antibody production. *Int. Immunopharmacol.* 54, 163–168 (2018).
- **In this work, gold nanoparticles of varying morphologies are used as adjuvants *in vivo* with antibody titers decreasing in the order of spheres, shells, stars and rods.**
- 49. Alaarg A, Senders ML, Varela-Moreira A *et al.* A systematic comparison of clinically viable nanomedicines targeting HMG-CoA reductase in inflammatory atherosclerosis. *J. Control Release* 262, 47–57 (2017).
- 50. Tian Y, Zhang J, Tang S, Zhou L, Yang W. Polypyrrole composite nanoparticles with morphology-dependent photothermal effect and immunological responses. *Small* 12(6), 721–726 (2016).
- 51. Du F, Liu Y-G, Scott EA. Immunotheranostic polymersomes modularly assembled from tetrablock and diblock copolymers with oxidation-responsive fluorescence. *Cel. Mol. Bioeng.* 10(5), 357–370 (2017).
- 52. Xing R, Li S, Zhang N, Shen G, Möhwald H, Yan X. Self-assembled injectable peptide hydrogels capable of triggering antitumor immune response. *Biomacromolecules* 18(11), 3514–3523 (2017).
- 53. Chen J, Pompano RR, Santiago FW *et al.* The use of self-adjuvanting nanofiber vaccines to elicit high-affinity B cell responses to peptide antigens without inflammation. *Biomaterials* 34(34), 8776–8785 (2013).
- 54. Zhang H, Park J, Jiang Y, Woodrow KA. Rational design of charged peptides that self-assemble into robust nanofibers as immune-functional scaffolds. *Acta Biomater.* 55, 183–193 (2017).
- 55. Chesson CB, Huelsmann EJ, Lacey AT *et al.* Antigenic peptide nanofibers elicit adjuvant-free CD8<sup>+</sup> T cell responses. *Vaccine* 32(10), 1174–1180 (2014).
- 56. Niikura K, Matsunaga T, Suzuki T *et al.* Gold nanoparticles as a vaccine platform: influence of size and shape on immunological responses *in vitro* and *in vivo*. *ACS Nano.* 7(5), 3926–3938 (2013).
- 57. Rudra JS, Banasik BN, Milligan GN. A combined carrier-adjuvant system of peptide nanofibers and toll-like receptor agonists potentiates robust CD8<sup>+</sup> T cell responses. *Vaccine* 36(4), 438–441 (2018).
- 58. Rudra JS, Khan A, Clover TM *et al.* Supramolecular peptide nanofibers engage mechanisms of autophagy in antigen-presenting cells. *ACS Omega* 2(12), 9136–9143 (2017).
- 59. Rodriguez PL, Harada T, Christian DA, Pantano DA, Tsai RK, Discher DE. Minimal “self” peptides that inhibit phagocytic clearance and enhance delivery of nanoparticles. *Science* 339(6122), 971–975 (2013).
- 60. Cherukula K, Nurunnabi M, Jeong YY, Lee Y-K, Park I-K. A targeted graphene nanoplatform carrying histamine dihydrochloride for effective inhibition of leukemia-induced immunosuppression. *J. Biomater. Sci. Polym. Ed.* 153, 1–16 (2017).
- 61. Han Q, Wang X, Jia X *et al.* CpG loaded MoS<sub>2</sub> nanosheets as multifunctional agents for photothermal enhanced cancer immunotherapy. *Nanoscale* 9(18), 5927–5934 (2017).
- 62. Zhang H, Yan T, Xu S *et al.* Graphene oxide-chitosan nanocomposites for intracellular delivery of immunostimulatory CpG oligodeoxynucleotides. *Mater. Sci. Eng. C* 73, 144–151 (2017).
- 63. Liu Z, Zhang S, Lin H *et al.* Theranostic 2D ultrathin MnO<sub>2</sub> nanosheets with fast responsibility to endogenous tumor microenvironment and exogenous NIR irradiation. *Biomaterials.* 155, 54–63 (2018).
- 64. Brewer MG, DiPiazza A, Acklin J, Feng C, Sant AJ, Dewhurst S. Nanoparticles decorated with viral antigens are more immunogenic at low surface density. *Vaccine* 35(5), 774–781 (2017).
- 65. Lee EJ, Nam G-H, Lee NK *et al.* Nanocage-therapeutics prevailing phagocytosis and immunogenic cell death awakens immunity against cancer. *Adv. Mater.* 30(10), doi: 10.1002/adma.201705581 (2018) (Epub ahead of print).
- 66. Guo X, Jin X, Lv X, Pu Y, Bai F. Real-time visualization of perylene nanoclusters in water and their partitioning to graphene surface and macrophage cells. *Environ. Sci. Technol.* 49(13), 7926–7933 (2015).
- 67. Li H, Fierens K, Zhang Z *et al.* Spontaneous protein adsorption on graphene oxide nanosheets allowing efficient intracellular vaccine protein delivery. *ACS Appl. Mater. Interfaces* 8(2), 1147–1155 (2016).
- 68. Witt KC, Castillo-Menendez L, Ding H *et al.* Antigenic characterization of the human immunodeficiency virus (HIV-1) envelope glycoprotein precursor incorporated into nanodiscs. *PLOS ONE.* 12(2), e0170672 (2017).



69. Ding P, Zhang T, Li Y *et al.* Nanoparticle orientationally displayed antigen epitopes improve neutralizing antibody level in a model of porcine circovirus type 2. *Int. J. Nanomed.* 12, 5239–5254 (2017).
70. Kuai R, Ochyl LJ, Bahjat KS, Schwendeman A, Moon JJ. Designer vaccine nanodiscs for personalized cancer immunotherapy. *Nat. Mater.* 16(4), 489–496 (2016).
71. Bowers DT, Olingy CE, Chhabra P *et al.* An engineered macroencapsulation membrane releasing FTY720 to precondition pancreatic islet transplantation. *J. Biomed. Mater. Res.* 106(2), 555–568 (2017).
72. Yang J, Shim S-M, Nguyen TQ *et al.* Poly- $\gamma$ -glutamic acid/chitosan nanogel greatly enhances the efficacy and heterosubtypic cross-reactivity of H1N1 pandemic influenza vaccine. *Sci. Rep.* 7, 44839 (2017).
73. Karabin NB, Allen S, Kwon H-K *et al.* Sustained micellar delivery via inducible transitions in nanostructure morphology. *Nat. Commun.* 9(1), 624 (2018).
74. Burke SE, Eisenberg A. Kinetics and mechanisms of the sphere-to-rod and rod-to-sphere transitions in the ternary system PS310-b-PAA52/Dioxane/Water. *Langmuir* 17(21), 6705–6714 (2001).
75. Lund R, Pipich V, Willner L, Radulescu A, Colmenero J, Richter D. Structural and thermodynamic aspects of the cylinder-to-sphere transition in amphiphilic diblock copolymer micelles. *Soft Matter* 7(4), 1491 (2011).
76. Rizwan SB, McBurney WT, Young K *et al.* Cubosomes containing the adjuvants imiquimod and monophosphoryl lipid A stimulate robust cellular and humoral immune responses. *J. Control Release.* 165(1), 16–21 (2013).
77. Bobbala S, Allen SD, Scott EA. Flash nanoprecipitation permits versatile assembly and loading of polymeric bicontinuous cubic nanospheres. *Nanoscale* 30(9), 267 (2017).